Dalton Transactions

PAPER

View Article Online
View Journal | View Issue

Cite this: *Dalton Trans.*, 2015, **44**, 15697

A hydrothermally stable Zn(II)-based metal–organic framework: structural modulation and gas adsorption†

Xiuling Zhang,[a] Yong-Zheng Zhang,[a] Da-Shuai Zhang,*[a] Baoyong Zhu[a] and Jian-Rong Li*[b]

By the solvothermal reaction of a triangular ligand, 2,4,6-tris-(4-carboxyphenoxy)-1,3,5-triazine (H_3tcpt) with $Zn(NO_3)_2{\cdot}6H_2O$ in *N*,*N*′-dimethylacetamide/acetonitrile/H_2O (v/v/v = 1 : 1 : 1) mixed solvents, a two-fold, interpenetrated, three-dimensional (3D), porous metal–organic framework, $[Zn_2(tcpt)OH]$·solvents (**1**·solvents), with a rare, paddlewheel secondary building unit (SBU), $Zn_2(COO)_3$, was synthesized and characterized. It was found that a single 3D structure of **1** forms when two-dimensional layers, which are constructed by $tcpt^{3-}$ bonding with the paddlewheel SBUs, are linked by –OH groups along the axial sites of the SBUs. Compared with the reported Zn(II)-based partners with this ligand, synthesis conditions, particularly the solvents used, clearly played a key role in the formation of different SBUs, thereby resulting in distinct MOFs with the same ligand. In particular, **1** features good water and thermal stability and can withstand acidic aqueous solutions with pH values ranging from 5 to 12. In addition, **1** displays good adsorption ability towards H_2 (2.21 wt% at 77 K and 1 atm) and can selectively adsorb CO_2 from CH_4 and N_2, in spite of its relatively low void volume (36.8%), suggesting potential applications in gas storage and separation.

Received 11th May 2015,
Accepted 24th July 2015

DOI: 10.1039/c5dt01770j

www.rsc.org/dalton

1. Introduction

As emerging porous materials, metal–organic frameworks (MOFs) have been widely researched over a number of years. Due to their interesting and varied structures and excellent chemical/physical properties, MOFs could be utilized in numerous areas, such as gas storage, separation, catalysis, magnetism, and luminescence.[1] However, to apply MOFs in practice, there are still many issues to be resolved; among them the stability of frameworks, especially under high temperatures and aqueous environment are significant. With this aim, some methods have been developed to enhance the stability of MOFs such as surface carbonization,[2] fluorine-modified pores,[3] and the construction of multi-interpenetrated frameworks.[4] Because MOFs are composed of organic linkers and secondary building units (SBU), the regulation of the two parts is vital for forming stable structures. Considering that the selection of organic linkers is relatively controllable, modulating the *in situ* formed SBUs is a conceivable way for enhancing the stability. On the other hand, the formation of a SBU depends on various factors,[5–7] *e.g.* reaction temperature, solvents, and pH. Under different conditions, MOFs with different structures and properties can be obtained.

In our efforts to design and synthesize new MOFs through controlling reaction conditions, we used a tritopic ligand, 2,4,6-tris-(4-carboxyphenoxy)-1,3,5-triazine (H_3tcpt), reported by several other groups for synthesizing MOFs.[6,7] From the literature, it was found that this ligand could generate a two-dimensional (2D) layered structural MOF, ($[Zn_3(L)_2(H_2O)_2]{\cdot}3H_2O{\cdot}$TEA·2DMF),[6] with $Zn_3(COO)_6$ SBUs in a mixed DMF/EtOH/H_2O solvent. The 2D layers could be linked by *in situ* produced formate species to form a three-dimensional (3D) framework (SNU-100)[7] when the solvent was changed to pure DMF. Clearly, solvents play a key role in the formation of these MOFs.

In this study, we used DMA/acetonitrile/H_2O (v/v/v = 1 : 1 : 1) as solvents and a new 3D MOF, $[Zn_2(tcpt)OH]$·solvents (**1**·solvents), was synthesized, in which an unusual paddlewheel SBU, $Zn_2(COO)_3$, was found. Unlike common paddlewheel SBUs[6–8] that consist of four carboxyl groups, this SBU has only three. Unlike the two above-mentioned MOFs, with this ligand,

[a]*Key Laboratory of Coordination Chemistry, Functional Materials in Universities of Shandong (Dezhou University), Dezhou, 253023 P. R. China. E-mail: dashuai_74@163.com*
[b]*Beijing Key Laboratory for Green Catalysis and Separation and Department of Chemistry and Chemical Engineering, Beijing University of Technology, Beijing 100124, P. R. China. E-mail: jrli@bjut.edu.cn*

†Electronic supplementary information (ESI) available. CCDC 1414115. For ESI and crystallographic data in CIF or other electronic format see DOI: 10.1039/c5dt01770j

in **1** the 2D layers assembled by H_3tcpt ligands and $Zn_2(COO)_3$ SBUs are further linked by –OH groups to finally form a 3D interpenetrated framework with excellent stability. Moreover, **1** displays good adsorption ability towards H_2 (2.21 wt% at 77 K and 1 atm) and can selectively adsorb CO_2 from CH_4 and N_2, in spite of its relatively low void volume (36.8%), suggesting its potential applications in gas storage and separation.

2. Experimental section

2.1 Materials and measurements

The ligand 2,4,6-tris(4-carboxyphenoxy)-1,3,5-triazine (H_3tcpt) was synthesized according to a method described in the literature.[9] All the commercially available chemicals and solvents were of reagent grade and were used as received without further purification. IR spectra were recorded on a Thermo Nicolet IR200 FT-IR spectrometer using KBr pellets (4000–400 cm^{-1}). Thermogravimetric analyses (TGA) were carried out on a SHIMADZU DTG-60 thermoanalyzer under nitrogen at a heating rate of 5 °C min^{-1} from room temperature to 700 °C. Powder X-ray diffraction (PXRD) measurements were performed on a SHIMADZU XRD-6000 X-ray diffractometer using Cu-Kα radiation (λ = 0.1542 nm), in which the X-ray tube was operated at 40 kV and 40 mA at room temperature. Temperature-dependent X-ray powder diffraction patterns were recorded on a Bruker D8 diffractometer at 40 kV and 40 mA with a Cu-target tube and a graphite monochromator. Elemental analysis for C, H and N was performed on an Elementar Vario Micro Cube analyzer. N_2, H_2, CO_2 and CH_4 adsorption measurements (up to 1 bar) were performed on an Autosorb-3.0 (Quantachrome) volumetric analyzer. All these gases were of extra-pure quality (99.999% purity).

2.2 Synthesis of 1·solvents

$Zn(NO_3)_2{\cdot}6H_2O$ (0.2 mmol, 59.4 mg) and H_3tcpt (0.1 mmol, 48.9 mg) were added to a mixed solvent of *N*,*N*′-dimethylacetamide (DMA)/acetonitrile (ACN)/H_2O (v/v/v = 1 : 1 : 1, 6 mL) with two drops of tetrafluoroboric acid (HBF_4, 48%) in a sealed glass vial. Then, the obtained mixture was ultrasonicated to dissolve and then heated at 90 °C for 48 h. After cooling to room temperature, prismatic colorless crystals were collected by filtration and washed with H_2O and DMA (Yield: 43.5% based on H_3tcpt). Anal. calcd (%) for the activated sample (see below) $C_{24}H_{13}N_3O_{10}Zn_2$ (%): C, 45.46; H, 2.07; N, 6.63. Found: C, 45.51; H, 2.01; N, 6.57.

2.3 X-ray crystallography

Diffraction intensity data of a single crystal of the complex was collected on an Agilent Technologies SuperNova diffractometer at 100 K equipped with a mirror monochromated Cu-Kα radiation (λ = 1.54184 Å) using a ω-scan mode. Empirical absorption correction using spherical harmonics was implemented in a SCALE3 ABSPACK scaling algorithm.[10] All the structures were solved by direct methods and refined by full-matrix least-squares methods on F^2 using the program SHELXL-2014.[11] The single suite WINGX[12] and Olex2 1.2-alpha[13] were used as integrated systems for the crystallographic programs. All non-hydrogen atoms were refined anisotropically. The hydrogen atoms were located by geometrical calculations and their positions and thermal parameters were fixed during the structure refinement. For this compound, the volume fractions of disordered solvent in the pores could not be modeled in terms of atomic sites and were treated using the MASK routine in the Olex2 software package. The coordination O atoms of hydroxy in **1**·solvents were disordered and treated by occupancies refinement of the disordered atoms. Crystallographic data and refinement parameters are listed in Table S1,† and selected bond lengths and angles are listed in Table S2.† CCDC 1414115 contains the supplementary crystallographic data of **1**.

2.4 Water stability test

Seven as-synthesized bulk samples in the same batch (45 mg) were soaked in aqueous solutions with pH = 5, 6, 7, 8, 9, 11, and 12 for 48 h. Subsequently, the samples were collected by decanting and dried in air, and then the structural integration was checked.

2.5 Gas adsorption measurement

Before gas adsorption measurements, the as-synthesized **1**·solvents was soaked in methanol for 3 days to exchange the solvents involved (DMA, ACN and H_2O). Subsequently, the sample was soaked in anhydrous dichloromethane for more than 3 days; during that time fresh dichloromethane was exchanged every day to completely remove methanol. The sample was collected by decanting and dried in air. Before the gas adsorption tests, the dry sample was loaded in a sample tube and further activated under high vacuum at an optimized temperature of 100 °C for 6 h. Finally, 68 mg of degassed sample was used for gas sorption measurements. The gas adsorption isotherm measurements were proceeded at 77 K in a liquid nitrogen bath, at 87 K in a liquid argon bath, at 195 K in a dry ice-acetone bath, at 273 K in an ice-water bath and at 298 K in a water bath.

3. Results and discussion

3.1 Synthesis and crystal structure

It is well-known that there are a lot of factors that can affect the formation of MOFs such as reaction solvent, temperature and pH. As shown in Scheme 1, three different MOFs were synthesized using the H_3tcpt ligand under different reaction conditions. $[Zn_3(tcpt)(H_2O)_2]{\cdot}3H_2O{\cdot}$TEA·2DMF, obtained by Han,[6] is an *AB* packing 2D structure with 41.4% void volume, while SNU-100, obtained by Suh,[7] possesses an interpenetrated 3D framework with 38.1% solvent accessible volume. In our study, **1** with a new structural type that is different from those of the above-mentioned two MOFs was obtained through a solvothermal reaction of $Zn(NO_3)_2{\cdot}6H_2O$ and H_3tcpt in a mixed solvent of DMA/ACN/H_2O with two drops of HBF_4 at 90 °C.

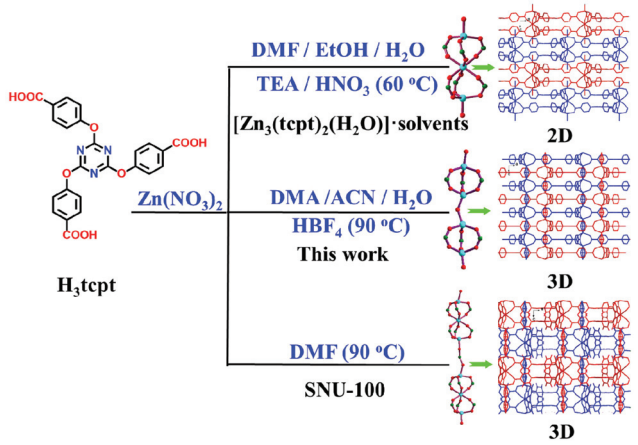

Scheme 1 Synthetic procedures and structures of three MOFs with H_3tcpt ligands obtained under different reaction conditions.

Single-crystal X-ray structural analysis reveals that **1**·solvents crystallizes in the hexagonal $P6_3/m$ space group and possesses a two-fold interpenetrated 3D framework structure. In the structure of **1**, there exists one crystallographically independent Zn(II) center, which is coordinated by three O atoms of carboxylate from three $tcpt^{3-}$ ligands and one O atom of hydroxy (Fig. 1a), and the angle between the triazine ring and the benzene ring in $tcpt^{3-}$ ligand is 90°. As shown in Fig. 1b, two adjacent Zn(II) ions are bonded together by three carboxylate groups to generate a paddlewheel SBU ($Zn_2(COO)_3$), which is linked by two hydroxy groups to obtain a five-connected node, as confirmed by solid state ^{1}H NMR (Fig. S7†). This node is different from the six-connected SBU node ($Zn_3(COO)_6$) in SNU-100[7] and $[Zn_3(tcpt)(H_2O)_2]\cdot 3H_2O\cdot$TEA·2DMF MOFs.[6] The Zn–O1 bond length is 1.921(4) Å, which is close to those reported in other zinc–carboxylate compounds.[5a,6,7,8b,c] In **1**, each SBU links to three $tcpt^{3-}$ ligands, and each $tcpt^{3-}$ ligand binds three SBUs to form a 2D layer with an irregular hexagonal lattice, which runs parallel to the *ab* plane. Interestingly, these 2D layers are linked by O atoms of hydroxy along the *c* axis, which gives rise to a 3D framework (Fig. 1c). Due to the large void, two 3D networks mutually interpenetrate (Fig. 1d), reinforcing each other *via* intermolecular π···π (3.4490 Å) interactions between the nearly coplanar central triazine rings. As a result, the stability of the whole framework is further enhanced (as discussed below) and the porosity of this MOF is tuned owing to the hexagonal channels being parted into three smaller rhombic channels with dimensions of about 4.0 × 6.4 Å (*a* × *b*, taking into account the van der Waals radii). By simplifying the organic ligand and the SBU as 3-connected and 5-connected nodes, respectively, the overall structural framework of **1** can be described as a (3,5)-connected infinite 3D *hms* topology (Schlafli symbol $(6^3)(6^9\cdot 8)$) (Fig. 1e). In addition, the effective free void volume of **1** is estimated to be about 36.8% (617.4 Å^3 out of the 1678.3 Å^3 per unit cell volume).

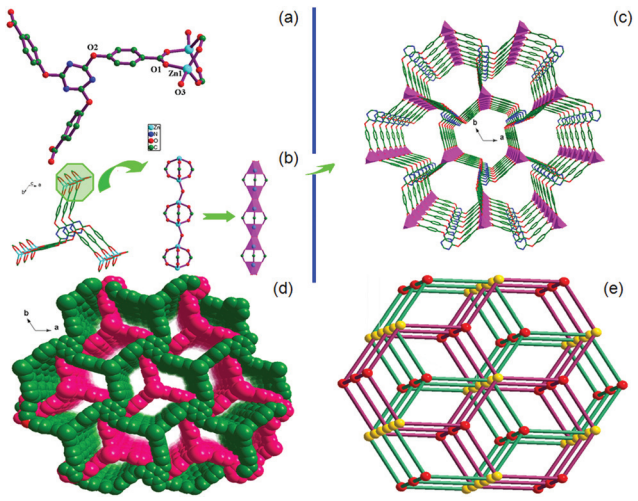

Fig. 1 (a) Coordination environment of Zn^{2+} in **1** (all H atoms have been omitted for clarity). (b) The localized geometry of $(Zn_2(COO)_3)$ SBU in **1** and polyhedral views of SBU. (c) View of the hexagonal one-dimensional (1D) channels in a single 3D framework of **1**. (d) Space-filling view of 1D channels in **1** (after interpenetration). (e) Schematic representation of the (3,5) topological net in **1**; the golden balls represent the three-connected ligand $tcpt^{3-}$ and the red balls represent the five-connected SBUs.

3.2 Stability

Framework stability is one of the restrictive factors for the practical application of MOFs. To examine the thermal and water stability of **1**, TGA and PXRD experiments were carried out. The TGA curve of the as-synthesized **1**·solvents reveals a total weight loss of 19.4% up to 400 °C, corresponding to the loss of the guest ACN, H_2O and DMA solvent molecules (calculated, 18.7%) followed by the decomposition of the compound (a significant weight loss is observed here) (Fig. S2b†). The TGA curve of the solvent (MeOH and CH_2Cl_2) exchanged sample of **1** exhibits a weight loss of 20% from 25 to 140 °C, indicating the removal of the new solvent molecules, and the framework remained stable up to 400 °C, followed by the decomposition of the compound. Compared with the 2D structural $[Zn_3(tcpt)(H_2O)_2]\cdot 3H_2O\cdot$TEA·2DMF[6] with a thermal stability up to 360 °C, SNU-100[7] and **1** appear to be more stable. This might be caused by the SBU stabilization.[28,29] In the SBU, Zn(II) is four-coordinated in a tetrahedral environment, which is generally a stable configuration for Zn(II) complexes. Moreover, both the discrete SBUs in SNU-100 and **1** were connected to form an infinite chain of linked SBUs, further improving the stability of the SBU and the whole frameworks.

It should be noted that a lot of MOFs cannot preserve their framework structures in water environment because the relatively weak coordination bonds could not withstand attack from water molecules, particularly in acidic/basic conditions, which limits their applications in a lot of fields. Therefore, stable MOFs are urgent pursuit.[14] For **1**, first it was found that the PXRD patterns of the as-synthesized bulk product, the solvent exchanged sample and the sample after gas-sorption

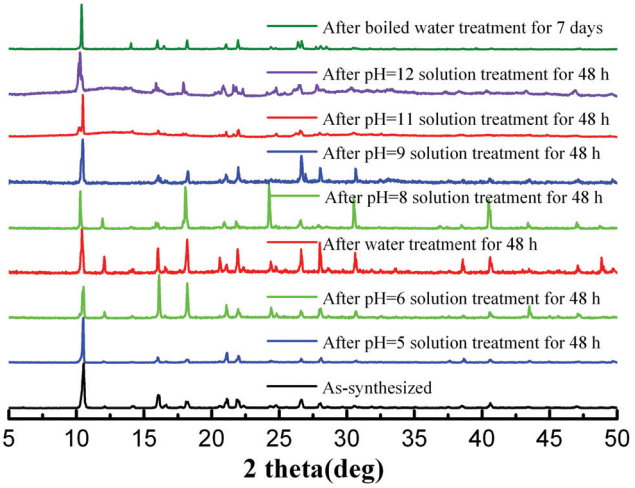

Fig. 2 PXRD patterns of **1** after being treated by soaking its samples in aqueous solutions of pH = 5, 6, 7, 8, 9, 11 and 12 for 48 h and boiled water for 7 days.

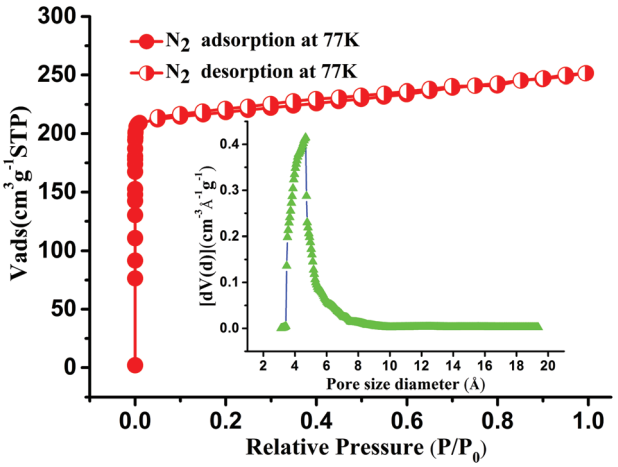

Fig. 3 N_2 sorption isotherms of **1** at 77 K (inset, pore size distribution plot).

are closely coincident with the simulated pattern derived from the X-ray single crystal data (Fig. S2a†), suggesting that this MOF has good stability against organic solvents and vacuum. Then, the PXRD patterns of samples of **1** that were treated by soaking in aqueous solutions of pH = 5, 6, 7, 8, 9, 11 and 12 for 48 h were collected (Fig. 2). Interestingly, the resulting patterns still matched well with the simulated ones, indicating high water stability even in the presence of acid. However, the samples of **1** dissolved in an aqueous solution with the pH greater than 13. Another tough condition, soaking samples of **1** in boiling water, was tested. Surprisingly, this MOF was stable in boiling water for at least 7 days, as proved by PXRD (Fig. 2 and S2e†). Furthermore, CO_2 uptake by samples of **1** treated with aqueous solutions with different pH values showed no obvious changes when compared with the original sample (Fig. 5d), also confirming the excellent framework stability of **1**. The excellent water/acid stability of this MOF may be attributed to the specific SBU and interpenetrated nature of its structure, being superior to many Zn(II)-based MOFs.

3.3 Gas adsorption

Encouraged by its porous structure, high stability and structural rigidity, a N_2 adsorption experiment at 77 K was performed to evaluate the porosity of **1**. The uptake of N_2 was 252 $cm^3\ g^{-1}$ (STP) at 77 K and 1 atm, and the adsorption isotherm showed a reversible type I isotherm (Fig. 3), which is characteristic of microporous material. The calculated H–K (Horvath–Kawazoe)[15] pore size distributions range from 3.2 to 7.8 Å, corresponding to the pore sizes evaluated from the single-crystal X-ray structure. Based on the N_2-adsorption isotherm, the Brunauer–Emmett–Teller (BET) and Langmuir surface areas of this MOF are estimated to be 905 and 1076 $m^2\ g^{-1}$, respectively, and the pore volume is 0.306 $cm^3\ g^{-1}$; all these values are higher than those for $Zn_3(tcpt)(H_2O)_2$.

The permanent porosity and suitable pore size in **1** prompted us to investigate its H_2 storage ability. The adsorption isotherms of H_2 at 77 and 87 K under pressures of up to 1 atm are shown in Fig. 4. These isotherms reveal that **1** can adsorb a large amount of H_2 up to 2.21 wt% and 1.52 wt%, respectively, at 1 atm. It should be noted that the H_2 uptake of **1** is comparable with that of many reported MOFs such as MOF-177,[S6] MOF-650,[S13] SNU-100′-M′,[7] and Cu_2(TPPC-O^{n}Pr),[S14] in spite of its relatively lower void volume (36.8%) and BET surface areas (Table S3†). It is noteworthy that the micropore size distribution of **1** is around 5 Å, which is close to the size of two H_2 molecules (2 × 2.8 Å), which may help in enhancing the interaction forces between the H_2 molecules and the framework, thereby benefiting H_2 adsorption. Moreover, as shown in Fig. S6,† interpenetration resulted in rhombic channels with small open windows (3.66 Å, Fig. S6†), which might

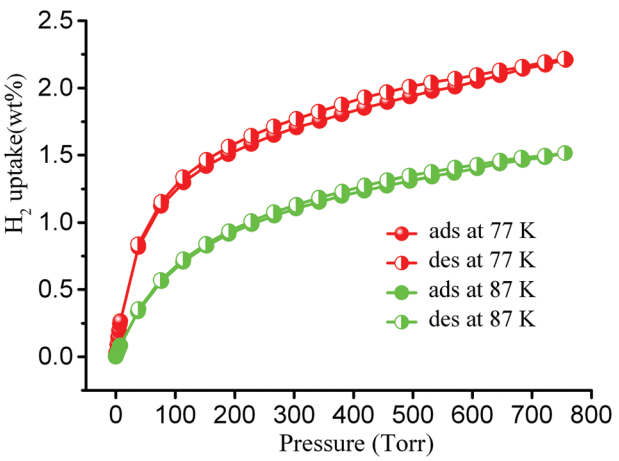

Fig. 4 H_2 sorption isotherms of **1**.

be beneficial for H_2 adsorption.[7,29,30] Some studies have proved that small pore size is necessary to achieve high H_2 uptake, because the small pore enables the overlap of energy potentials between the opposing walls, leading to a higher interaction energy with H_2 molecules.[31–34] For example, PCN-6 exhibits a higher H_2 uptake than PCN-6′, indicating a substantially stronger interaction in the interpenetrated PCN-6, than that in the non-interpenetrated PCN-6′.[35] To evaluate the interaction between the adsorbed H_2 molecules and the host framework of **1**, the isosteric heats of adsorption (Q_{st}) of H_2 adsorption were calculated and were found to be 8.0–6.8 kJ mol^{-1}, depending on the degree of H_2 loading (Fig. S3b†); these were estimated by fitting the H_2 isotherms at 77 and 87 K using a virial method (Fig. S3a†).[16] The initial Q_{st} (8.0 kJ mol^{-1}) is higher than those for some common MOFs such as MOF-5 (4.8 kJ mol^{-1}) because of the small pore size that result from the structural interpenetration.

Although non-interpenetrated frameworks usually have large pores and high surface areas, which are suitable for a lot of adsorption-based applications,[8a,S6,S13] the interpenetrated networks have been proven to be useful in some cases such as in selective guest capture.[4b,17–20] Therefore, **1** was further checked for CO_2, CH_4 and N_2 capture. The adsorption isotherm of CO_2 at 195 K is shown in Fig. 5a. Clearly, significant amounts of CO_2 were adsorbed, and the isotherm presented a typical type I curve with no obvious change after repeated cycling. The adsorption amounts increase abruptly over the low pressure range, up to 150 $cm^3\ g^{-1}$ (STP) at 50 torr, and finally up to 205 $cm^3\ g^{-1}$ (40.3 wt%) at 1 atm. Approximately, 11.6 CO_2 molecules are adsorbed for per cell volume of **1**. Moreover, as shown in Fig. 5b and c, gas adsorptions of **1** exhibit significantly different uptakes towards CO_2, CH_4 and N_2 at both 273 and 298 K. **1** can uptake a moderate amount of CO_2 up to 110.5 $cm^3\ g^{-1}$ (273 K) and 71.3 $cm^3\ g^{-1}$ (298 K), while the uptake amounts of CH_4 are 45.8 $cm^3\ g^{-1}$ (273 K) and 19.9 $cm^3\ g^{-1}$ (298 K) at 1 atm. However, at the two temperatures, the uptake amounts of N_2 are only 17.7 and 3.5 $cm^3\ g^{-1}$, respectively, at 1 atm.

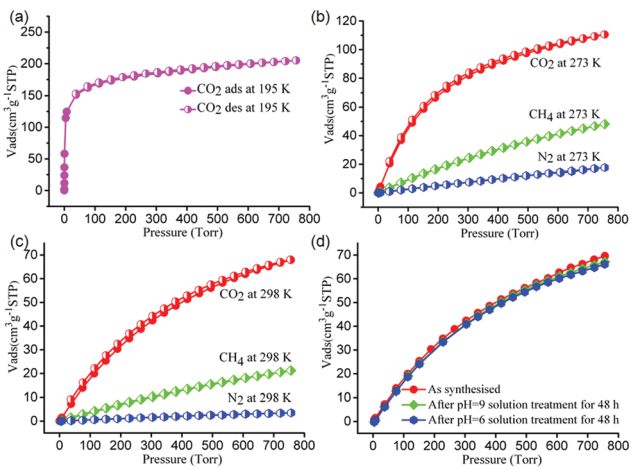

Fig. 5 Gas sorption isotherms for **1**: (a) CO_2 at 195 K. (b) CO_2, CH_4 and N_2 at 273 K. (c) CO_2, CH_4 and N_2 at 298 K. (d) CO_2 at 298 K.

To estimate the adsorption selectivities of **1** towards CO_2, CH_4 and N_2, the initial slopes of their adsorption isotherms were calculated over very low pressure ranges (Fig. S5a and b†).[21] The calculated CO_2/CH_4 selectivity is 5.2 : 1 at 273 K and 5.0 : 1 at 298 K. Using the same method, the CO_2/N_2 selectivities were calculated to be 19.4 : 1 at 273 K and 33.6 : 1 at 298 K. The selectivity for CO_2 over N_2 at 298 K is indeed comparable to some reported MOFs (Table S4†) and higher than BPL carbon, which is widely applied in industry for gas separations.[36] In addition, to evaluate the interaction between CO_2 molecules and the host framework, CO_2 isosteric heats of adsorption (Q_{st}) in **1** were calculated based on the respective adsorption isotherms at 273 K and 298 K. Employing the Clausius–Clapeyron equation,[22,23] the calculated Q_{st} values range from 31.2 to 40.9 kJ mol^{-1}, depending on the gas loading (Fig. S4†). The observed selective sorption behaviors of CO_2 over CH_4 and N_2 may be attributed to the stronger host–guest interaction between the CO_2 molecules with large quadrupole moment and the framework, as compared with the other two gases.[24–27] On the other hand, the framework interpenetration leads to narrow rhombic channels with a size of 4.0 × 6.4 Å. However, the height of the rhombic channels is only 3.66 Å (Fig. S6†). Given the dynamic radius of these gas molecules, namely, CO_2 (3.3 Å), N_2 (3.64 Å), and CH_4 (3.8 Å), a dimensional effect may also play an important role for selective adsorption.

4. Conclusions

A novel, two-fold interpenetrated 3D MOF with a rare Zn(II)-based SBU, ($Zn_2(COO)_3$), has been synthesized under solvothermal reaction conditions and characterized structurally. Compared with the reported Zn(II)-based partners with the same ligand, the synthesis conditions, particularly the solvents used, played a key role in the formation of different SBUs, thereby producing distinct MOFs in this system. In particular, **1** has good thermal and excellent water stability, even in acidic aqueous solution with pH ranging from 5 to 12. In addition, **1** has adequate gas sorption capabilities for H_2 and CO_2 and high adsorption selectivities towards CO_2 over N_2 and CH_4, suggesting its potential applications in gas storage and separation.

Acknowledgements

This study was financially supported by the National Science Foundation of China (21371028).

References

1 (*a*) J. Liu, P. K. Thallapally, B. P. McGrail, D. R. Brown and J. Liu, *Chem. Soc. Rev.*, 2012, **41**, 2308; (*b*) S.-S. Chen,

P. Wang, S. Takamizawa, T.-A. Okamura, M. Chen and W.-Y. Sun, *Dalton Trans.*, 2014, **43**, 6012; (*c*) J. Yang, X. Wang, R. Wang, L. Zhang, F. Liu, F. Dai and D. Sun, *Cryst. Growth Des.*, 2014, **14**, 6521; (*d*) K. Na, K. M. Choi, O. M. Yaghi and G. A. Somorjai, *Nano Lett.*, 2014, **14**, 5979; (*e*) T. Panda, T. Kunduz and R. Banerjee, *Chem. Commun.*, 2012, **48**, 5464; (*f*) M. Zhu, S.-Q. Su, X.-Z. Song, Z.-M. Hao, S.-Y. Song and H.-J. Zhang, *Dalton Trans.*, 2012, **41**, 13267; (*g*) Y.-X. Ren, X.-J. Zheng, L.-C. Li, D.-Q. Yuan, M. An and L.-P. Jin, *Inorg. Chem.*, 2014, **53**, 12234; (*h*) T. Aharen, F. Habib, I. Korobkov, T. J. Burchell, R. Guillet-Nicolas, F. Kleizb and M. Murugesu, *Dalton Trans.*, 2013, **42**, 7795; (*i*) J.-R. Li, Q. Yu, E. C. Sanudo, Y. Tao and X.-H. Bu, *Chem. Commun.*, 2007, 2602.

2 (*a*) S. J. Yang and C. R. Park, *Adv. Mater.*, 2012, **24**, 4010; (*b*) D. Bradshaw, A. Garai and J. Huo, *Chem. Soc. Rev.*, 2012, **41**, 2344.

3 (*a*) C. Yang, U. Kaipa, Q. Z. Mather, X. Wang, V. Nesterov, A. F. Venero and M. A. Omary, *J. Am. Chem. Soc.*, 2011, **133**, 18094; (*b*) D.-S. Zhang, Z. Chang, Y.-F. Li, Z.-Y. Jiang, Z.-H. Xuan, Y.-H. Zhang, J.-R. Li, Q. Chen, T.-L. Hu and X.-H. Bu, *Sci. Rep.*, 2013, **3**, 3312.

4 (*a*) Y.-Q. Chen, G.-R. Li, Z. Chang, Y.-K. Qu, Y.-H. Zhang and X.-H. Bu, *Chem. Sci.*, 2013, **4**, 3678; (*b*) Y. He, Z. Zhang, S. Xiang, F. R. Fronczek, R. Krishna and B. Chen, *Chem. Commun.*, 2012, **48**, 6493.

5 (*a*) X. Zhao, H. He, F. N. Dai, D. Sun and Y. Ke, *Inorg. Chem.*, 2010, **49**, 8650; (*b*) Z. Wang, B. Zheng, H. Liu, P. Yi, X. Li, X. Yu and R. Yun, *Dalton Trans.*, 2013, **42**, 11304; (*c*) A. K. Chaudhari, S. S. Nagarkar, B. Joarder and S. K. Ghosh, *Cryst. Growth Des.*, 2013, **13**, 3716; (*d*) H. He, F. Sun, T. Borjigin, N. Zhao and G. Zhu, *Dalton Trans.*, 2014, **43**, 3716.

6 L. Han, Y. Yan, F. X. Sun, K. Cai, B. Borjigin, X. Zhao, F. Qu and G. Zhu, *Cryst. Growth Des.*, 2013, **13**, 1458.

7 H. J. Park and M. P. Suh, *Chem. Sci.*, 2013, **4**, 685.

8 (*a*) S. Zhang, Z. Chang, T.-L. Hu and X.-H. Bu, *Inorg. Chem.*, 2010, **49**, 11581; (*b*) M.-S. Chen, M. Chen, T. Okamura, W.-Y. Sun and N. Ueyama, *Microporous Mesoporous Mater.*, 2011, **139**, 25; (*c*) Z.-Q. Shi, Z.-J. Guo and H.-G. Zheng, *Chem. Commun.*, 2015, **51**, 8300.

9 C. B. Aakeroy, J. Desper and J. F. Urbina, *CrystEngComm*, 2005, **7**, 193.

10 *CrysAlis RED*, Oxford Diffraction Ltd., Version 1.171.29.2.

11 G. M. Sheldrick, *Acta Crystallogr., Sect. C: Cryst. Struct. Commun.*, 2015, **71**, 3–8.

12 L. J. Farrugia, *J. Appl. Crystallogr.*, 1999, **32**, 837.

13 O. V. Dolomanov, L. J. Bourhis, R. J. Gildea, J. A. K. Howard and H. J. Puschmann, *J. Appl. Crystallogr.*, 2009, **42**, 339–341.

14 (*a*) J. Yang, A. Grzech, F. M. Mulderb and T. J. Dingemans, *Chem. Commun.*, 2011, **47**, 5244; (*b*) J. J. Low, A. I. Benin, P. Jakubczak, J. F. Abrahamian, S. A. Faheem and R. R. Willis, *J. Am. Chem. Soc.*, 2009, **131**, 15834; (*c*) H. Jasuja and K. S. Walton, *Dalton Trans.*, 2013, **42**, 15421; (*d*) J. H. Im, N. Ko, S. J. Yang, H. J. Park, J. Kim and C. R. Park, *New J. Chem.*, 2014, **38**, 2752.

15 G. Horvath and K. Kawazoe, *Chem. Eng. Jpn.*, 1983, **16**, 470.

16 L. Czepirski and J. JagieLlo, *Chem. Eng. Sci.*, 1989, **44**, 797.

17 Y.-W. Li, L.-F. Wang, K.-H. He, Q. Chen and X.-H. Bu, *Dalton Trans.*, 2011, **40**, 10319.

18 S.-Q. Ma, X.-S. Wang, E. S. Manis, C. D. Collier and H.-C. Zhou, *Inorg. Chem.*, 2007, **46**, 3432.

19 H. Kim and M. P. Suh, *Inorg. Chem.*, 2005, **44**, 810.

20 S. Bureekaew, H. Sato, R. Matsuda, Y. Kubota, J. Kim, K. Kato, M. Takata and S. Kitagawa, *Angew. Chem., Int. Ed.*, 2010, **49**, 7660.

21 J. An, S. J. Geib and N. L. Rosi, *J. Am. Chem. Soc.*, 2010, **132**, 38.

22 D. Zhong, J. Lin, W. Lu, L. Jiang and T. Lu, *Inorg. Chem.*, 2009, **48**, 8656.

23 M. Dincă and J. R. Long, *J. Am. Chem. Soc.*, 2005, **127**, 9376.

24 J.-R. Li, J. Sculley and H.-C. Zhou, *Chem. Rev.*, 2012, **112**, 869.

25 Y. Qin, X. Feng, F. Luo, G. Sun, Y. Song, X. Tian, H. Huang, Y. Zhu, Z. Yuan, M. Luo, S. Liu and W. Xu, *Dalton Trans.*, 2013, **42**, 50.

26 J.-B. Lin, J.-P. Zhang and X.-M. Chen, *J. Am. Chem. Soc.*, 2010, **132**, 6654.

27 J. Lincke, D. Lässig, M. Kobalz, J. Bergmann, M. Handke, J. Möllmer, M. Lange, C. Roth, A. Möller, R. Staudt and H. Krautscheid, *Inorg. Chem.*, 2012, **51**, 7579.

28 D. Sun, Y. Ke, D. J. Collins, G. A. Lorigan and H.-C. Zhou, *Inorg. Chem.*, 2007, **46**, 2725.

29 D. Zhao, D. J. Timmons, D. Yuan and H.-C. Zhou, *Acc. Chem. Res.*, 2010, **44**, 123.

30 L. Pan, M. B. Sander, X. Huang, J. Li, M. Smith, E. Bittner, B. Boclrath and J. K. Johnson, *J. Am. Chem. Soc.*, 2004, **126**, 1308.

31 M. P. Suh, H. J. Park, T. K. Prasad and D.-W. Lim, *Chem. Rev.*, 2012, **112**, 782.

32 D. H. Everett and J. C. Powl, *J. Chem. Soc., Faraday Trans.*, 1976, **72**, 619.

33 D. Zhao, D. Yan and H.-C. Zhou, *Energy Environ. Sci.*, 2008, **1**, 225.

34 B. Kesanli, Y. Cui, M. R. Smith, E. W. Bittner, B. C. Bockrath and W. Lin, *Angew. Chem., Int. Ed.*, 2005, **44**, 72.

35 (*a*) S.-Q. Ma, D. Sun, M. Ambrogio, J. A. Fillinger, S. Parkin and H.-C. Zhou, *J. Am. Chem. Soc.*, 2007, **129**, 1858; (*b*) S.-Q. Ma, J. Eckert, P. M. Forster, J. W. Yoon, Y. K. Hwang, J.-S. Chang, C. D. Collier, J. B. Parise and H.-C. Zhou, *J. Am. Chem. Soc.*, 2008, **130**, 15896.

36 M. G. Nijkamp, J. E. M. J. Raaymakers, A. P. van Dillen and K. P. de Jong, *Appl. Phys. A: Mater. Sci. Process.*, 2001, **72**, 619.

